Available online at www.sciencedirect.com
ScienceDirect
Journal of Contaminant Hydrology 95 (2008) 121–140
JOURNAL OF Contaminant Hydrology
www.elsevier.com/locate/jconhyd

A new tracer technique for monitoring groundwater fluxes: The Finite Volume Point Dilution Method

Serge Brouyère [a,b,*], Jordi Batlle-Aguilar [a], Pascal Goderniaux [a,c], Alain Dassargues [a]

[a] Department ArGEnCo, Hydrogeology Unit, University of Liège, Building B52/3, 4000 Sart Tilman, Belgium
[b] Aquapôle, University of Liège, Building B52/3, 4000 Sart Tilman, Belgium
[c] National Funds for Scientific Research of Belgium, Belgium

Received 17 May 2007; received in revised form 16 August 2007; accepted 7 September 2007
Available online 15 September 2007

Abstract

Quantification of pollutant mass fluxes is essential for assessing the impact of contaminated sites on their surrounding environment, particularly on adjacent surface water bodies. In this context, it is essential to quantify but also to be able to monitor the variations with time of Darcy fluxes in relation with changes in hydrogeological conditions and groundwater — surface water interactions. A new tracer technique is proposed that generalizes the single-well point dilution method to the case of finite volumes of tracer fluid and water flush. It is called the Finite Volume Point Dilution Method (FVPDM). It is based on an analytical solution derived from a mathematical model proposed recently to accurately model tracer injection into a well. Using a non-dimensional formulation of the analytical solution, a sensitivity analysis is performed on the concentration evolution in the injection well, according to tracer injection conditions and well-aquifer interactions. Based on this analysis, optimised field techniques and interpretation methods are proposed. The new tracer technique is easier to implement in the field than the classical point dilution method while it further allows monitoring temporal changes of the magnitude of estimated Darcy fluxes, which is not the case for the former technique. The new technique was applied to two experimental sites with contrasting objectives, geological and hydrogeological conditions, and field equipment facilities. In both cases, field tracer concentrations monitored in the injection wells were used to fit the calculated modelled concentrations by adjusting the apparent Darcy flux crossing the well screens. Modelling results are very satisfactory and indicate that the methodology is efficient and accurate, with a wide range of potential applications in different environments and experimental conditions, including the monitoring with time of changes in Darcy fluxes.

Keywords: Tracer technique; Single well; Darcy flux; Experimental setup; Analytical solution

1. Introduction

In many practical applications in hydrogeology, it is necessary to estimate groundwater fluxes, or even to be able to monitor their evolution with time. For groundwater remediation, because of the concomitant and opposite effects of contaminant mobility and contaminant retardation or reaction, estimating Darcy fluxes and contaminant effective velocity in groundwater is essential for assessing the natural attenuation capacity of the subsurface (Valocchi, 1985; Brusseau, 1994; Li et al., 1994). Darcy fluxes are also required for dimensioning remediation systems such as reactive barriers, because their feasibility and efficiency mainly depend on the magnitude of

* Corresponding author. Department ArGEnCo, Hydrogeology Unit, University of Liège, Building B52/3, 4000 Sart Tilman, Belgium. Tel.: +32 43662377; fax: +3243669520.
E-mail address: Serge.Brouyere@ulg.ac.be (S. Brouyère).

0169-7722/$ - see front matter © 2007 Elsevier B.V. All rights reserved.
doi:10.1016/j.jconhyd.2007.09.001

groundwater and contaminant fluxes in the aquifer (e.g. Morrison et al., 2002; Hatfield et al., 2004). Recently, important research efforts have also been devoted to better understanding and quantifying, at local and catchment scales, the mechanisms that govern the interactions between groundwater and surface water. These mechanisms play an important role on riparian ecosystems, on the fate of trace metals and organic contaminants, particularly in the hyporheic zone and, from a more general perspective, they have to be well understood to efficiently protect and manage water resources (Kalbus et al., 2006). A good perception of hydrogeologic systems requires knowledge of the local groundwater flow paths, the rates of exchange between stream and groundwater and the dynamics of such exchanges with varying river stage conditions (Wroblicky et al., 1998; Arntzen et al., 2006).

The most basic approach to estimating groundwater fluxes is to use Darcy's law with estimates of hydraulic conductivity (e.g. from pumping tests) and hydraulic gradients. However, doing so provides a rough estimate of the Darcy flux, subject to large errors (Devlin and McElwee, 2007), and only valid at the scale of the distance between the observation wells used to calculate the hydraulic gradient or at the scale of the pumping test used to determine the hydraulic conductivity.

The Point Dilution Method — PDM (e.g. Havely et al., 1967; Drost et al., 1968; Klotz et al., 1978; Hall, 1996) allows to locally estimate groundwater fluxes based on the concentration decline monitored with time in an injection well. However, the injection is difficult to perform because the tracer must be instantaneously and uniformly mixed in the well bore water at the beginning of the test, without perturbation of the flow pattern around the well. Furthermore, this technique just provides an estimate of the Darcy flux at a given time, and it cannot be used to monitor changes in Darcy fluxes with time.

Recently, Brouyère (2003) presented a new mathematical and numerical approach to accurately model tracer injection into a well, considering injection conditions, such as the volume of tracer fluid and water flush, the flow rates or the injection duration and well-aquifer interactions, such as the flow rate that is actually crossing the screens due to motion of water in the aquifer. This model was used by Brouyère et al. (2005) in order to determine how and to what extent the tracer injection can influence the shape of the breakthrough curve and its interpretation. In that article, an analytical solution was derived and used to perform a detailed analysis of the evolution of the tracer input function in the aquifer for a better identification and understanding of factors that actually govern the influence of injection conditions on tracer test results.

Here, the same analytical solution is used to develop a new single-well tracer technique, called the Finite Volume Point Dilution Method (FVPDM) that generalizes the PDM to almost any kind of tracer injection scenario, and particularly to the case of a finite volume of tracer fluid and water flush. It can be used to locally estimate Darcy fluxes at the injection point for any type of tracer experiment. This new method allows for an easier experimental setup than the PDM and it has the further advantage over the PDM that it can be used for monitoring variations with time of the Darcy fluxes.

In the next chapters, the analytical solution obtained by Brouyère et al. (2005) is briefly reviewed, putting the accent on some mathematical aspects required to understand the specificity of the FVPDM. A non-dimensional formulation of the analytical solution is then used to perform a sensitivity analysis of the concentration evolution in the well during and after the tracer injection. Based on this analysis, several methodologies and interpretation formulas are proposed and discussed. The FVPDM technique was applied successfully in two case studies with contrasting scientific objectives and experimental conditions. The results of these experiments are used here to illustrate the adequacy and usefulness of the new tracer technique and to prove its applicability in the field. The potential for further developing the tracer technique to monitor transient Darcy fluxes, for example for changing river stage or piezometry, is also discussed.

2. The mathematical basis for FVPDM

The analytical solution obtained by Brouyère et al. (2005) for calculating the concentration evolution in the injection well is:

$$C_w(t) = \frac{Q_{\text{in}}C_{\text{in}} - \left(Q_{\text{in}}C_{\text{in}} - Q_{\text{out}}C_{w,0}\right)\exp\left(-\frac{Q_{\text{out}}}{V_w}(t-t_0)\right)}{Q_{\text{out}}} \tag{1}$$

with,

$$Q_{\text{out}} = Q_{\text{in}} + Q_t^{\text{in}} \tag{2}$$

In Eqs. (1) and (2), C_w, C_{in} and $C_w{}^0$ are tracer concentrations (M L^{-3}) in the well, in the injection water, and in the injection well at time t_0, respectively. The injection rate is Q_{in} (L^3 T^{-1}), Q_t^{in} (L^3 T^{-1}) is the rate of water intercepted by the well at the screen level (transit flow rate) and Q_{out} (L^3 T^{-1}) is the flow rate that leaves the well through the screens, carrying tracer at concentration C_w. The superscript 'in' in the transit flow rate Q_t^{in} indicates the fact that this flow rate dynamically depends on the injection rate Q_{in} (see next section).

The term $V_w=\pi r_w^2 h_w$ is the volume of water in the injection well, where h_w (L) and r_w (L) represent the height of the water column in the well bore and the radius of the injection well, respectively. The volume of water in the injection well is assumed to be constant. This assumption is valid if a packer system is used in the well to isolate the injection level from the rest of the well bore and if variations in water level are small compared to the height of the water column in the well. Furthermore, as discussed later, the FVPDM should be performed using a low injection rate, which increases the chances to keep a constant water level in the well.

Eq. (1) extends the classical PDM to the case of finite volumes of tracer fluid and finite duration of tracer injection. Because the PDM relies on limiting assumptions of an instantaneous injection and a complete mixing of tracer diluted into an infinitesimal volume of water, Eq. (1) is a major improvement since it generalizes the former technique to experimental conditions that are more realistic and easier to perform in the field (Brouyère, 2001).

2.1. Evaluation of the transit flow rate Q_t^{in}

The physical process behind the FVPDM is dilution by mixing of the different flow rate components (Q_{in} and Q_t^{in}), which is similar to the standard dilution technique commonly used in hydrology to calculate flow rates in streams (Gilman, 1977a,b; Australian Government, 2006; Ruehl et al., 2006).

The FVPDM is, however, more complex than the dilution technique because the relationship between the injection flow rate Q_{in} and the transit flow rate Q_t^{in} is non-linear, as it depends on the flow patterns around the injection well and on the well geometry. As explained in Brouyère (2003), the transit flow rate Q_t^{in} is maximum when the injection rate is equal to zero and it progressively decreases as the injection rate increases. For a critical value of the injection rate $Q_{in}=Q_{cr}$, the transit flow rate Q_t^{in} is exactly zero. Above the critical injection rate, only injection water leaves the well screen. This implies that the FVPDM should be performed with a tracer injection rate which is less than a critical injection rate (Q_{cr}) above which the transit flow rate crossing the screens of the injection well could not be determined because it would be cancelled. The key for developing the FVPDM is thus to accurately express the dependency of Q_t^{in} on Q_{in} and to evaluate as accurately as possible the critical injection rate (Q_{cr}).

Using the principle of superposition, Bidaux and Tsang (1991) developed equations to compute steady-state potential and stream functions near a well for purely regional flow, purely radial flow or a combination of both. Their equations allow calculation of Darcy flux components $v_r(r,\theta)$ and $v_\theta(r,\theta)$ in a (r,θ) coordinates system centred on the well (Fig. 1) and the output flow rate Q_{out} leaving the well screen. For the more general case of combined regional and radial flow, $v_r(r,\theta)$ and $v_\theta(r,\theta)$ are given by:

$$v_r(r,\theta) = -\hat{K}(r)\left[a(r)r^{\alpha(r)-1} - \frac{b(r)}{r^{\alpha(r)+1}}\right]\cos\theta + \frac{Q_{in}}{2\pi e_{scr} r_w} \quad (3a)$$

$$v_\theta(r,\theta) = \alpha(r)\hat{K}(r)\left[a(r)r^{\alpha(r)-1} + \frac{b(r)}{r^{\alpha(r)+1}}\right]\sin\theta \quad (3b)$$

where all coefficients are given in Bidaux and Tsang (1991).

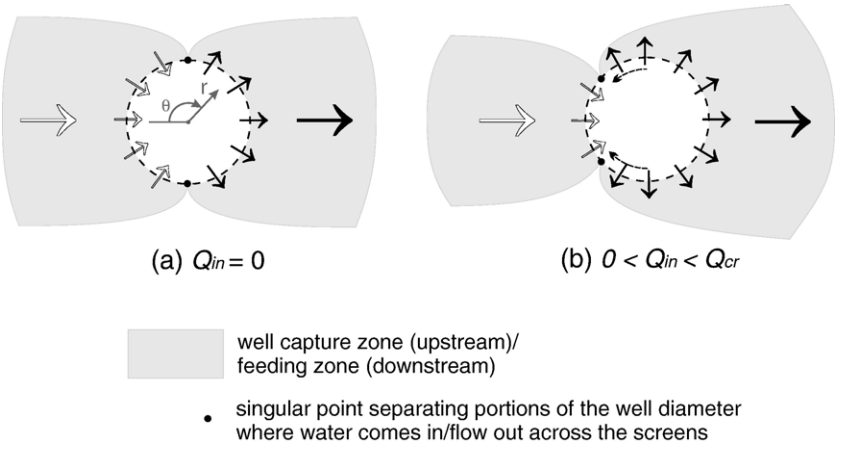

Fig. 1. Flow patterns around the injection well (a) in natural flow conditions, (b) modified by the injection of water in the well and radial coordinate system used to calculate the components of Darcy flux at the vicinity of the injection well (adapted from Brouyère, 2003).

At the well radius, the Darcy flux components ($L\,T^{-1}$) evaluated with expressions (3a) and (3b) are given by,

$$v_\theta(r_w,\theta)=0 \tag{4a}$$

$$v_r(r_w,\theta)=-v_{ap}\cos\theta+\frac{Q_{\text{in}}}{2\pi e_{\text{scr}} r_w} \tag{4b}$$

where $v_{ap}=\alpha_w|\underline{v}_D|$ is the apparent Darcy flux measured at the well, α_w is a non-dimensional correction factor (distortion coefficient), $|\underline{v}_D|$ is the magnitude of the mean Darcy flux ($L\,T^{-1}$) that would prevail close to the well in the absence of flow distortion, e_{scr} (L) is the screen length of the well and r_w (L) is the radius of the injection well.

If the hydraulic conductivity field is homogeneous, α_w reflects the possible distortion of the flow field around the injection well (Drost et al., 1968; Hall, 1996; Brouyère, 2003). The flux component for the θ coordinates is always equal to zero (Eq. (4a)) and the Darcy flux field is purely radial for all values of pumping or injection rate in the well.

The flow rate Q_{out} leaving the well can be evaluated using the expression for v_r (Eq. (4b)). The screen section through which water is leaving the well corresponds to values of θ where $v_r(r_w,\theta)>0$. In natural flow conditions, when the injection rate $Q_{\text{in}}=0$, Eq. (4b) gives the following inequality,

$$v_r(r_w,\theta)=-v_{ap}\,\cos\theta\geq 0 \tag{5}$$

which is valid if $\cos\theta\leq 0$, so if $\frac{\pi}{2}\leq\theta\leq\frac{3\pi}{2}$. Therefore, in the absence of any injection ($Q_{\text{in}}=0$), groundwater enters the well along the upstream segment of the screen which corresponds to, and leaves from the half downstream segment, as expected (Fig. 1a). The flow rate dq_{out} leaving the well between angles θ and $\theta+d\theta$ is given by:

$$dq_{\text{out}}=r_w e_{\text{scr}} v_r(r,\theta)d\theta=-r_w e_{\text{scr}} v_{ap}\cos\,\theta\,d\theta \tag{6}$$

Integrating Eq. (6) over half of the well circumference provides the following expression:

$$\begin{aligned} Q_{\text{out}}=Q_t^0&=\int_{\pi/2}^{3\pi/2} dq_{\text{out}}\\ &=r_w e_{\text{scr}}\int_{\pi/2}^{3\pi/2}\left(-v_{ap}\,\cos\,\theta\right)d\theta=2r_w e_{\text{scr}} v_{ap}\\ &=2r_w e_{\text{scr}}\alpha_w|\underline{v}_D| \end{aligned} \tag{7}$$

As expected, the flow rate leaving the well is the product between the apparent Darcy flux (v_{ap}) and the section of the injection well orthogonal to the main flow direction ($2r_w e_{\text{scr}}$).

For the more general case, when water is injected in the well at a rate $Q_{\text{in}}>0$ (Fig. 1b), the solution of Eq. (8) gives the portion of the well circumference where water leaves the well.

$$\cos\,\theta\leq\frac{Q_{\text{in}}}{2\pi r_w e_{\text{scr}} v_{ap}} \tag{8}$$

Because of the condition $-1\leq\cos\theta\leq 1$, for injected water, the bounding value $\cos\theta=1$ provides the mathematical expression for the critical injection rate (Q_{cr}):

$$Q_{\text{cr}}=2\pi r_w e_{\text{scr}} v_{ap}=2\pi r_w e_{\text{scr}}\alpha_w|\underline{v}_D| \tag{9}$$

For an injection rate $Q_{\text{in}}>Q_{\text{cr}}$, all water leaving the well through the screen is injected water, the transit water flow rate Q_t being exactly offset by the injection flow rate Q_{in}. Bidaux and Tsang (1991) draw the same conclusions by computing the stream function rather than Darcy fluxes at the well circumference.

A comparison of the natural transit flow rate Q_t^0 (Eq. (7)) and the critical injection rate Q_{cr} (Eq. (9)) shows that they are related as follows:

$$Q_{\text{cr}}=\pi Q_t^0 \tag{10}$$

The factor π simply comes from the difference between the flow section associated to these two flow rates, which is the well diameter ($2r_w$) for Q_t^0 and the well circumference ($2\pi r_w$) for Q_{cr}.

If $Q_{\text{in}}\leq Q_{\text{cr}}$, the cosine inequality (Eq. (8)) allows defining the portion of circumference where the water leaves the well:

$$\arccos\left(\frac{Q_{\text{in}}}{Q_{\text{cr}}}\right)\leq\theta\leq 2\pi-\arccos\left(\frac{Q_{\text{in}}}{Q_{\text{cr}}}\right) \tag{11}$$

Using the limits defined in Eq. (11), the flow rate Q_{out} leaving the well through the screen is given by:

$$\begin{aligned} Q_{\text{out}}&=\int_{\arccos Q_{\text{in}}^*}^{2\pi-\arccos Q_{\text{in}}^*}\left(-r_w e_{\text{scr}} v_{ap}\cos\theta+\frac{Q_{\text{in}}}{2\pi}\right)d\theta\\ &=2r_w e_{\text{scr}} v_{ap}\sin\left(\arccos\,Q_{\text{in}}^*\right)\\ &\quad+\frac{Q_{\text{in}}}{2\pi}\left(2\pi-2\,\arccos Q_{\text{in}}^*\right) \end{aligned} \tag{12}$$

where $Q_{\text{in}}^*=Q_{\text{in}}/Q_{\text{cr}}$

Finally, the expression for the transit flow rate is given by:

$$Q_t^{\text{in}} = Q_{\text{out}} - Q_{\text{in}} = 2r_w e_{\text{scr}} v_{ap} \sin\left(\arccos Q_{\text{in}}^*\right) - \frac{Q_{\text{in}}}{2\pi}\left(2 \arccos Q_{\text{in}}^*\right) \quad (13)$$

Using Eq. (13) assumes that the different flow rates (Q_{in}, Q_t^{in}, Q_{out}) reach equilibrium almost instantaneously during tracer injection, such that $Q_{\text{out}} = Q_{\text{in}} + Q_t^{\text{in}}$. This assumption is generally not valid if the injection rate is very high or if the hydraulic conductivity near the injection well is very low. However, with such injection rate or hydraulic conductivity, it is likely that the transit flow rate would be zero ($Q_{\text{in}}^* > 1$).

2.2. Non-dimensional formulation of the injection model

As shown by Brouyère et al. (2005), a more general form of Eq. (1) can be obtained using non-dimensional variables, by normalizing concentration, volume, flow rates and time variables according to the concentration in the tracer fluid C_{inj}, the volume of water in the injection well V_w, the critical injection flow rate Q_{cr} and the time T_w needed to replace the water in the well at this critical injection rate ($T_w = V_w/Q_{\text{cr}}$), respectively. The non-dimensional form of Eq. (1) can be written as:

$$C_w^*(t^*) = \frac{Q_{\text{in}}^* C_{\text{in}}^* - \left(Q_{\text{in}}^* C_{\text{in}}^* - Q_{\text{out}}^* C_{w,0}^*\right) \exp\left(-Q_{\text{out}}^* t^*\right)}{Q_{\text{out}}^*} \quad (14)$$

The following section presents a sensitivity analysis for the evolution of concentration in the injection well during and after tracer injection, based on non-dimensional Eq. (14). It will allow for a better understanding of practical conditions under which the new single-well tracer experiment has to be performed in order to obtain useful results and to propose interpretation methods and formulas. For the sake of generality, the non-dimensional formulation is used, but the methodology, the reasoning and the conclusions are valid for the corresponding dimensional variables as well.

3. Sensitivity analysis of the concentration evolution on tracer injection and local groundwater flow conditions

The most general way of performing a tracer injection is as follows. A quantity M_{inj} (M) of tracer is diluted in a volume V_{inj} (L^3) of water, at a concentration $C_{\text{in}} = C_{\text{inj}} = M_{\text{inj}}/V_{\text{inj}}$ ($M\ L^{-3}$). The tracer fluid is injected during a period T_{inj} (T) at an injection flow rate is $Q_{\text{in}} = Q_{\text{inj}} = V_{\text{inj}}/T_{\text{inj}}$ ($L^3\ T^{-1}$). Sometimes, the tracer injection is followed by a flush with clear (untraced) water ($C_{in} = 0$) to accelerate the transfer of the tracer from the injection well to the surrounding aquifer. This flush is performed with a volume of water V_{fl} (L^3), injected over a period T_{fl}, at an injection rate $Q_{\text{in}} = Q_{\text{fl}} = V_{\text{fl}}/T_{\text{fl}}$ ($L^3\ T^{-1}$). When tracer injection and subsequent flushing are completed, some tracer remains in the injection well, from where it is progressively released in the aquifer, as a result of the transit flow rate Q_t^0 ($L^3\ T^{-1}$) crossing the well screens in natural flow conditions. Table 1 summarizes the dimensional and the non-dimensional terms for the different possible steps of tracer injection operations. In the following section, the evolution of concentration in the injection well during the various phases of tracer injection is performed and analysed to propose in the next section the most efficient methodology for the FVPDM.

3.1. Concentration evolution during tracer injection

If one assumes that, at the beginning of tracer injection, there is no tracer in the well ($C_{w,0}^* = 0$) and that appropriate values are used for the flow rate variables (see Table 1), Eq. (14) can be written:

$$C_w^*(t^*) = \frac{Q_{\text{inj}}^*\left(1 - \exp\left(-Q_{\text{out}}^* t^*\right)\right)}{Q_{\text{out}}^*} \quad (15)$$

The concentration evolution in the injection well $C_w^*(t^*)$, as computed according to Eq. (15), is presented in Fig. 2. Each continuous curve corresponds to a constant injection rate Q_{inj}^*, moving along a curve corresponding to increasing tracer volumes V_{inj}^* and injection durations t_{inj}^*. Concentrations increase for larger injection rates and longer injection duration, thus for larger injection volumes.

The curve $C_w^*(Q_{in}^* = 1)$ divides the diagram into two contrasting domains. If the injection rate is higher than the critical injection rate ($Q_{\text{inj}}^* > 1$, Fig. 2, domain 1), the concentration in the well approaches the concentration in the injected tracer fluid ($C_w^* \rightarrow 1$) when the volume of tracer is large ($V_{\text{inj}}^* \approx 5$). If the injection rate is lower than the critical injection rate ($Q_{\text{inj}}^* < 1$, Fig. 2, domain 2), the concentration in the well never approaches that in the injected tracer fluid ($C_w^* < 1$), whatever the volume of tracer fluid injected because the transit flow rate crossing the screens contributes to tracer dilution in the well. In this case, provided that the injection duration is long enough, the concentration in the well approaches a value $C_{w,\text{stab}}^*$ which is all the lower as the injection rate is low, thus as the transit flow rate is high.

Table 1
Dimensional and non-dimensional values taken by the different variables for the different phases of the tracer injection process

Dimensional variables					
	C_{in}	V_{in}	Q_{in}	Q_t^{in}	Q_{out}
Tracer injection	C_{inj}	V_{inj}	Q_{inj}	Q_t^{inj}	$Q_{inj}+Q_t^{inj}$
Tracer flush	0	V_{fl}	Q_{fl}	Q_t^{fl}	$Q_{fl}+Q_t^{fl}$
Natural release of the tracer	0	0	0	Q_t^0	Q_t^0
Non-dimensional variables					
	$C_{in}^* = C_{in}/C_{inj}$	$V_{in}^* = V_{in}/V_w$	$Q_{in}^* = Q_{in}/Q_{cr}$	$Q_t^{in*} = Q_t^{in}/Q_{cr}$	$Q_{out}^* = Q_{out}/Q_{cr}$
Tracer injection	$C_{inj}^*=1$	V_{inj}^*	Q_{inj}^*	Q_t^{inj*}	$Q_{inj}^* + Q_t^{inj*}$
Tracer flush	0	V_{fl}^*	Q_{fl}^*	Q_t^{fl*}	$Q_{fl}^*+Q_t^{fl*}$
Natural release of the tracer	0	0	0	$Q_t^{0*}=1/\pi$	$Q_t^{0*}=1/\pi$

The stabilized concentration level in the well can be computed as follows:

$$C_{w,stab}^* = \lim_{t_{inj}^* \to \infty} \left(\frac{Q_{inj}^* \left(1 - \exp\left(-Q_{out}^* t_{inj}^*\right)\right)}{Q_{out}^*} \right) = \frac{Q_{inj}^*}{Q_{out}^*} = \frac{Q_{inj}^*}{Q_{inj}^* + Q_t^{in*}} = \frac{Q_{inj}}{Q_{inj} + Q_t^{in}} \quad (16)$$

From a practical point of view, Eq. (16) allows estimation of the transit flow rate Q_t^{in} by performing a low-rate tracer injection of long duration, which is as close to the natural transit flow rate Q_t^0 as the injection rate is low (see practical examples in the next section).

In Fig. 2, the dotted lines correspond to envelope curves of the maximum concentration reached in the well at the end of tracer injection, for variable tracer volumes V_{inj}^*. If $Q_{inj}^* \geq 1$ (Fig. 2, domain 1), the concentration reached in the well at the end of tracer injection is independent of the injection duration t_{inj}^* (concentration plateau at the beginning of each envelope curve). If $Q_{inj}^* < 1$ (Fig. 2, domain 2), the concentration level reached in the well at the end of tracer injection decreases with the injection duration t_{inj}^*. In the first case, the transit flow rate is cancelled and the only contribution to tracer dilution comes from the mixing between untraced water initially present in the well bore (V_w) and the tracer fluid (V_{inj}), quantified by the mixing factor $V_{inj}^* = V_{inj}/V_w$. In the second case, the

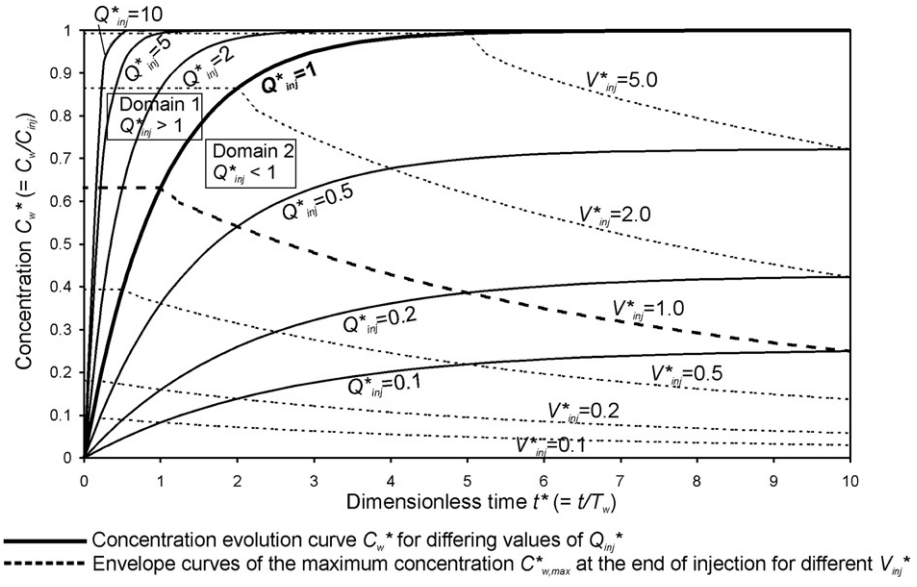

Fig. 2. Dimensionless representation of concentration evolution in the well according to injection conditions.

existing transit flow rate also contributes to tracer dilution in the well bore.

These observations can be obtained mathematically using Eq. (15), by calculating the concentration in the well at the end of tracer injection (for $t^*=t^*_{\mathrm{inj}}$):

For $Q^*_{\mathrm{inj}}>1$, $C^*_{\mathrm{inj}}=1$, $C^*_{w,0}=0$, $Q^*_{\mathrm{out}}=Q^*_{\mathrm{inj}}$ and $Q^*_{\mathrm{inj}}t^*_{\mathrm{inj}}=V^*_{\mathrm{inj}}$:

$$C^*_{w,e_{\mathrm{inj}}}=\frac{Q^*_{\mathrm{inj}}\left(1-\exp\left(-Q^*_{\mathrm{out}}t^*_{\mathrm{inj}}\right)\right)}{Q^*_{\mathrm{out}}}=1-\exp\left(-V^*_{\mathrm{inj}}\right) \tag{17a}$$

For $Q^*_{\mathrm{inj}}<1$, $Q^*_{\mathrm{out}}=Q^*_{\mathrm{inj}}+Q_t^{\mathrm{inj}*}$:

$$C^*_{w,e_{\mathrm{inj}}}=\frac{Q^*_{\mathrm{inj}}\left(1-\exp\left(-\left(V^*_{\mathrm{inj}}+Q_t^{\mathrm{inj}*}t^*_{\mathrm{inj}}\right)\right)\right)}{Q^*_{\mathrm{out}}}=\frac{Q^*_{\mathrm{inj}}\left(1-\exp\left(-\left(V^*_{\mathrm{inj}}+V^*_t\right)\right)\right)}{Q^*_{\mathrm{out}}} \tag{17b}$$

In Eq. (17a), $C^*_{w,e_{\mathrm{inj}}}$ depends only on the mixing factor V^*_{inj}. In Eq. (17b), $C^*_{w,e_{\mathrm{inj}}}$ still depends on the mixing factor V^*_{inj}, but also on the transit flow rate $Q_t^{\mathrm{inj}*}$ and on the injection duration t^*_{inj}, with the product $Q_t^{\mathrm{inj}*}t^*_{\mathrm{inj}}=V_t^*$ being the volume of groundwater that flows across the well screen during tracer injection. This means that the rising part, as well as the stabilized part of the concentration evolution in the injection well can be used to evaluate Q_t^{inj} and Q_t^0 provided that $Q_{\mathrm{inj}}<Q_{\mathrm{cr}}$. As mentioned already, Q_t^{inj} is calculated using Eq. (13), knowing the injection rate Q_{inj}.

If $Q_{\mathrm{inj}}\geq Q_{\mathrm{cr}}$, thus if $Q^*_{\mathrm{inj}}\geq 1$, $Q_{\mathrm{out}}=Q_{\mathrm{inj}}$ and Eq. (17a) allows one to check if the mixing volume of water V_w^{mix}, defined as the volume of water actually involved in the injection and mixing processes, differs from the actual volume of water stored in the well bore $V_w=\pi r_w^2 h_w$ (i.e. based on the geometry of the well). Discrepancies can be expected between V_w^{mix} and V_w. A smaller mixing volume of water may be expected if the mixing procedure does not involve the whole column of water in the well. On the contrary, a bigger mixing volume of water may be observed if either the well casing is deteriorated or if groundwater located around the well is directly involved in the mixing process.

3.2. Concentration evolution after tracer injection

When the injection of the tracer fluid is completed, a water flush is frequently performed in the well by injecting untraced water ($C^*_{\mathrm{fl}}=C_{\mathrm{fl}}/C_{\mathrm{inj}}=0$) at a rate Q_{fl} to accelerate the transfer of the tracer from the well into the aquifer around. During this phase, Eq. (14) can be written:

$$C^*_w=C^*_{w,0}\ \exp\left(-Q^*_{\mathrm{out}}t^*\right) \tag{18}$$

where $C^*_{w,0}$ is the non-dimensional concentration in the well at the beginning of the flush (usually at the end of the tracer fluid injection).

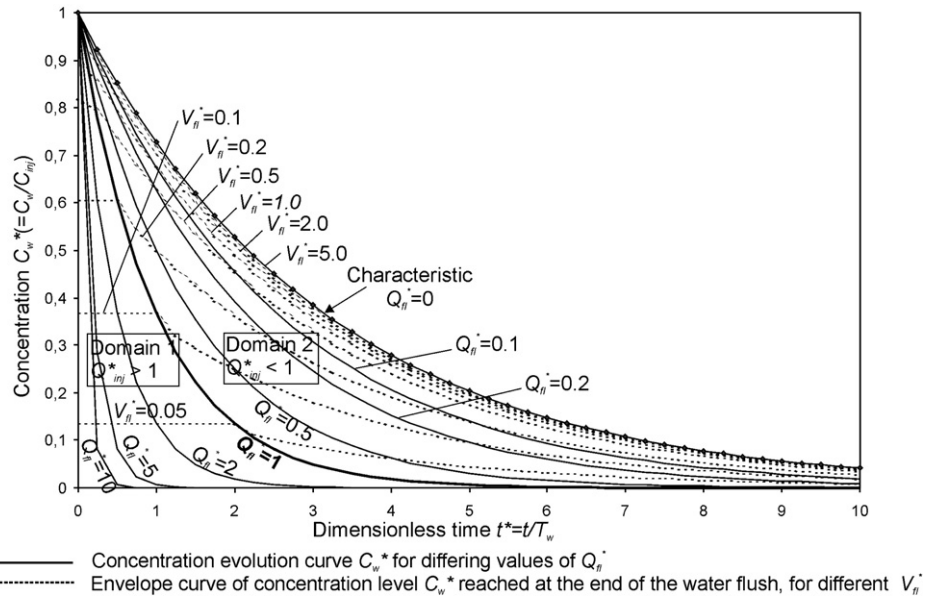

Fig. 3. Dimensionless graphical representation of concentration evolution in the well during water flush or natural release of the tracer.

Eq. (18) expresses that the concentration in the injection well decreases exponentially, at a rate which is proportional to $Q^*_{out}=Q^*_{fl}+Q_t^{fl*}$.

The concentration evolution in the well during the flush, as computed with Eq. (18), is presented in Fig. 3, assuming $C^*_{w,0}=1$ at the beginning of the water flush. The time scale refers to the beginning of the flush. Each continuous curve corresponds to a constant flush rate Q^*_{fl}, moving along a curve corresponding to increasing water flush volumes V^*_{fl} and flush durations t^*_{fl}. Concentrations decrease for higher flushing rates and longer flush duration or larger flush volumes. In a semi-log diagram (t, $\log C^*_w$), these curves would plot as straight lines of negative slope equal to Q^*_{out}.

The dotted lines correspond to envelop curves of the concentration reached in the well at the end of the flush, for variable flush volumes V^*_{fl}. If $Q^*_{fl}>1$ (Fig. 3, domain 1), the concentration level $C^*_{w,e_{fl}}$, reached in the well at the end of the flush, depends only on the flush mixing factor $V^*_{fl}=V_{fl}/V_w$ (and on the initial concentration in the well $C^*_{w,0}$). If $Q^*_{fl}<1$ (Fig. 3, domain 2), $C^*_{w,e_{fl}}$ decreases with the flush duration (t^*_{fl}).

These observations can be obtained mathematically from Eq. (18), by calculating the concentration in the well at the end of the tracer flush (for $t^*=t^*_{fl}$):

If $Q^*_{fl}>1$, $Q^*_{out}=Q^*_{fl}$, thus $Q^*_{fl}t^*_{fl}=V^*_{fl}$ and,

$$C^*_{w,f_{fl}} = C^*_{w,0}\ \exp\left(-Q^*_{fl}t^*_{fl}\right) = C^*_{w,0}\ \exp\left(-V^*_{fl}\right) \quad (19a)$$

If $Q^*_{fl}<1$, $Q^*_{out}=Q^*_{fl}+Q_t^{fl*}$ and,

$$C^*_{w,e_{fl}} = C^*_{w,0}\ \exp\left(-\left(V^*_{fl}+Q_t^{fl*}t^*_{fl}\right)\right) \quad (19b)$$

As for the equivalent case during tracer injection, if $Q^*_{fl}\geq 1$, $Q_{out}=Q_{fl}$, and Eq. (19a) allows one to check if the mixing volume of water in the well V_w^{mix} differs from the actual volume of water V_w located in the well bore.

If $Q_{fl}<Q_{cr}$, Eq. (19b) can be used to calculate the total flow rate Q_{out} leaving the well through the screens, thus the transit flow rate Q_t^{fl} crossing the screens during the water flush:

$$Q_t^{fl} = -\frac{\Delta_{ch}V_w}{\log e} - Q_{fl} \quad (20)$$

where Δ_{ch} is the slope of the decrease of concentration plotted in a semi-log diagram (t, $\log C^*_w$) and $\log e=0{,}43429$.

If a flush is not performed ($Q^*_{fl}=0$), the tracer is flushed from the well because of the transit flow rate Q_t^{0*} crossing the screens in natural flow conditions. This comes to the interpretation formula used for the classical point dilution method.

$$C^*_w(t^*) = C^*_{w,e_{inj}}\ \exp\left(-Q_t^{0*}t^*\right) = C^*_{w,e_{inj}}\ \exp\left(-t^*/\pi\right) \quad (21)$$

where $C^*_{w,f}$ is the concentration of the tracer remaining in the well at the end of the injection.

4. Field applications

The Finite Volume Point Dilution Method was applied in two case studies. The results obtained during these experiments are used here to show the accuracy of the mathematical concepts and of the analytical solution on which the tracer technique relies. More information about these experiments is available in technical reports (Batlle-Aguilar and Brouyère, 2005, 2006; Goderniaux and Brouyère, 2006).

The first case study consists in tracer experiments between piezometers and a spring line system in a small (11.7 km^2) catchment located in the north west of France (Val d'Oise — Brévilles springs). The saturated aquifer is located in sandy layers overlain by unsaturated fractured marly limestones (unsaturated zone). The objectives of the tracer experiments were to highlight vertical variations in mostly horizontal groundwater fluxes in the sandy aquifer, related to vertical variations in grain size distribution and hydraulic conductivity, to estimate contaminant travel times from several locations in the catchment to the Brévilles springs and to identify transport processes affecting the fate of solute contaminants in the saturated part of the aquifer. Considering these objectives, monitoring the concentration evolutions at the injection points was performed (1) to check that the tracers did not remain captured close to the injection point, as discussed in Brouyère et al. (2005), (2) to obtain local estimates of Darcy fluxes in the aquifer, which is a useful complementary information with regards to the general objectives of the experiments.

The field conditions in Brévilles did not offer the possibility of obtaining a power supply, an unlimited quantity of water and a protection of the equipment against vandalism. These conditions did not allow to apply the most advanced experimental setup of the FVPDM, as described further in section 4.1. Long-duration tracer injections were not possible and the tests had to be dimensioned in a "shorter version". For each test, only the beginning of the rising concentration curves was monitored and modelled, using several steps of increasing injection rates. Furthermore, due to recovery

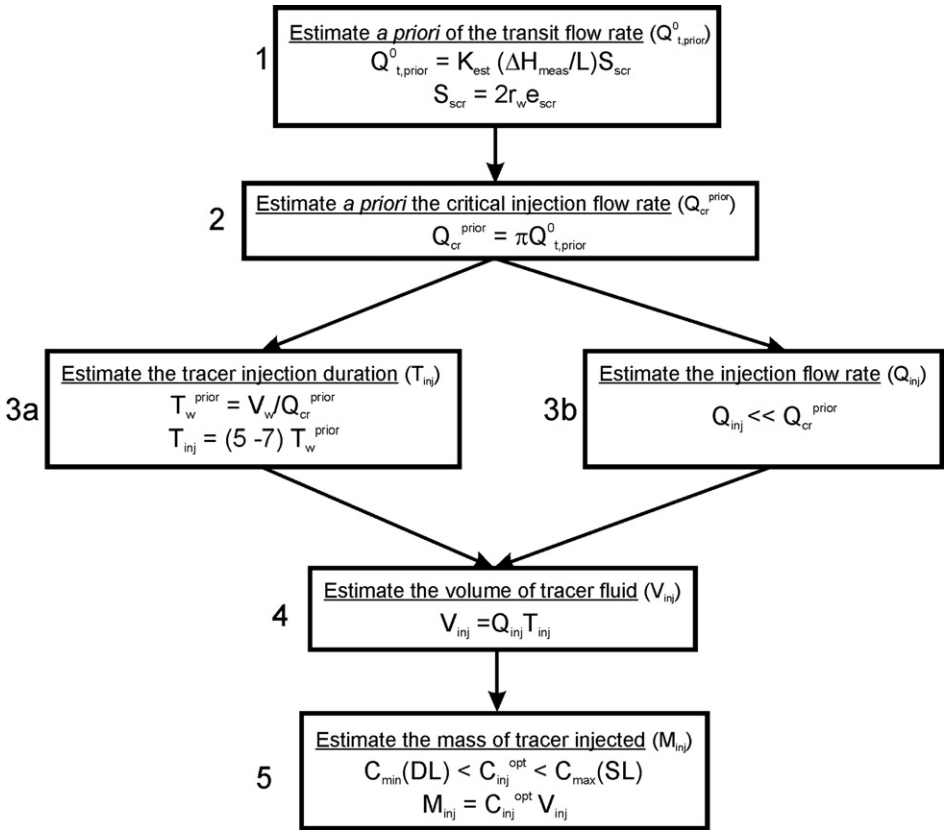

Fig. 4. Flowchart for the definition of the optimal FVPDM injection profile.

objectives at the Brévilles spring, the required quantity of tracer was large and the resulting high concentrations in the injection tracer fluid made handling operations less comfortable.

The second test site (further called site A) is a brownfield of 7.3 ha corresponding to a former cokery. It is located 30 m from the Meuse River, on the north bank, upstream of the city of Liège, Belgium. Groundwater is contaminated by inorganic (mainly sulphates and heavy metals) and organic pollutants (BTEX and PAH). The main objective of the tracer experiments was to evaluate groundwater fluxes discharging in the Meuse River. It was decided to apply the FVPDM in several observation wells located at the boundary of the site, near the river. At this site, the experimental conditions allowed to define and to use the most adequate and sophisticated experimental setup for monitoring tracer experiments over a long period so as to optimize the chances of reaching stabilization of concentration in the injection wells.

In the following sections, the FVPDM methodology, as used in actual field practice, is described first. After a brief description of the tracer experiments performed in the two contrasting experimental sites, modelling results of the concentration evolutions using Eq. (1) are presented and discussed.

4.1. The FVPDM as performed in the field

Generally, the objectives of the study and the conditions prevailing in the field are the main constraining factors for dimensioning the tracer experiments, which will be illustrated by the results of the two case studies presented here. However, based on the theory, it is possible to propose a very structured methodology for dimensioning the FVPDM experiment prior to going to the field. This is summarized in Fig. 4 in the form of a flowchart which is described in details below.

As already mentioned, an essential condition for the FVPDM to be valid is that the injection rate should be less than the critical injection rate ($Q^*_{inj}<1$). If that condition is not met, the concentration in the injection well (C_w) would become equal to the concentration of the injected tracer (C_{inj}) and the monitored evolution of concentration in the well could not provide an estimation of Darcy fluxes in the vicinity of the well.

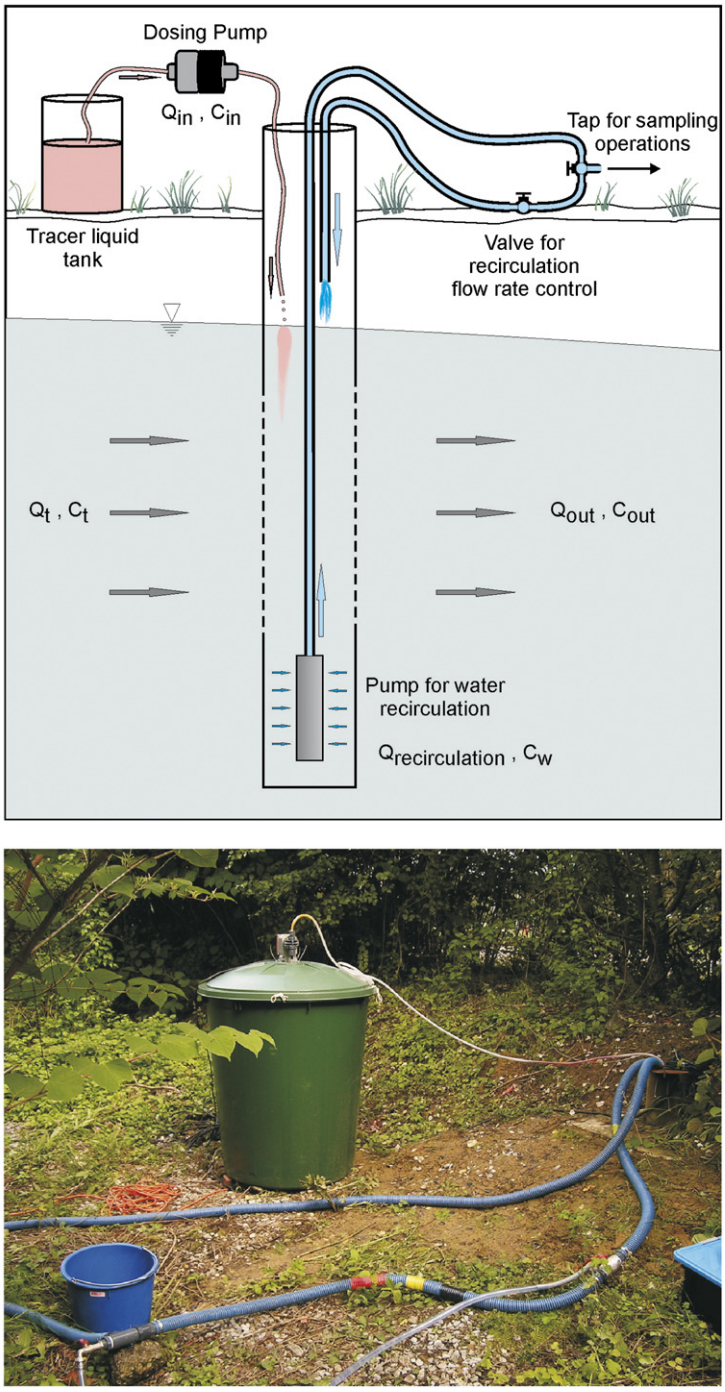

Fig. 5. Schematic experimental device (above) and real experimental device in the field (below).

The first step in setting up the experiment is thus to estimate *a priori* the critical injection rate Q_{cr} by applying Darcy's law with estimated hydraulic conductivity and hydraulic gradient (Fig. 4, step 1). Values of hydraulic conductivity and hydraulic gradient can be obtained from pumping test results and from groundwater levels measured in the vicinity of the injection well, respectively.

When the critical injection rate Q_{cr} is estimated from Q_t (Fig. 4, step 2), one can define the injection profile

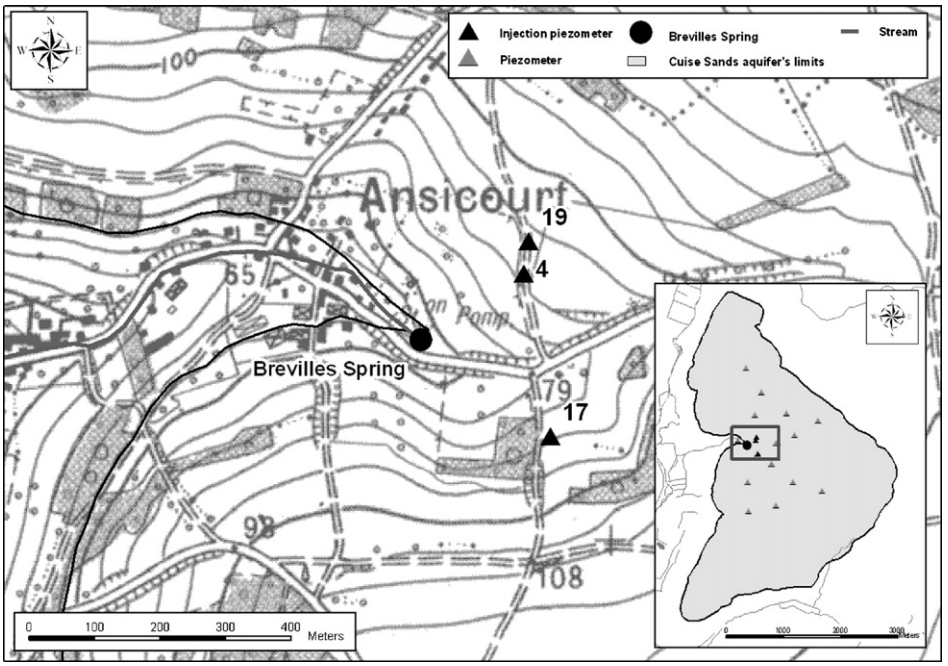

Fig. 6. Global view of the Brévilles test site and detail of the spring area (injection area).

(Q_{inj}, V_{inj}, T_{inj}, C_{inj},…) as follows. Theoretically, a single injection step at a constant rate Q_{inj} is sufficient to obtain a concentration evolution that is useful for the FVPDM interpretation. Here, it was however decided to perform, for each injection, various injection steps with increasing injection rates, the idea being to check that the relationship between Q_t^{inj} and Q_{inj} remains valid for different values of Q_{inj}. It can also be expected that the resulting multi-step concentration evolution can provide a more reliable estimation of Darcy fluxes. Using increasing injection rates reduces also the risk of injecting the tracer at a rate that is larger than the critical injection rate.

Based on Fig. 2, one can estimate that the concentration evolution in the injection well stabilizes after a minimal injection duration T_{inj} equal to five times T_w. Knowing Q_{cr} and V_w, one can estimate T_w and then T_{inj} (Fig. 4, step 3a). At the same time, the prior estimate of Q_{cr} allows one to define an optimal value of Q_{inj}, as low as possible as compared to Q_{cr} (Fig. 4, step 3b). Having defined Q_{inj} and T_{inj} allows then to determine the volume of tracer fluid V_{inj} (Fig. 4, step 4).

The quantity of tracer has to be defined so as to have concentrations in the injection fluid (C_{inj}) and in the injection well (C_w) that are higher than the detection limit ($C_{inj} > C_{DL}$), to be easily detected and monitored, but still low enough to avoid adverse problems such as saturation of monitoring devices or density effects ($C_{inj} < C_{SL}$). So, the final step consists in defining the quantity of tracer M_{inj} such that concentrations in the injection fluid C_{inj} and in the injection well C_w are within this acceptable interval (Fig. 4, step 5). During the experiment, 'real-time' measurements of the electrical conductivity or the fluorescence is recommended to monitor "on-line" the concentration evolution and to check that the injection rate remains lower than the critical injection rate ($Q_{inj} < Q_{cr}$). Of course, if the FVPDM is performed in conjunction with another tracer experiment, like in Brévilles (see after), the quantity of tracer should be defined such that the tracer is likely to be recovered at the downstream monitoring point(s) in the aquifer.

Fig. 5 shows the basic experimental devices and their layout in the field. At each site, the tracer was injected using a peristaltic pump for injection rates lower than 3.4 l/h or a dosing pump for injection rates up to 40 l/h. Groundwater circulation was performed in each injection well in order to homogenize the tracer concentration in the well and to obtain samples at the injection point. This was accomplished using an immersed pump, with a circulation rate ranging between 0.3 and 3 m^3/h.

4.2. Experimental validation in a small catchment (Brévilles, France)

The aquifer of the Brévilles spring is located in the Val d'Oise (France), 80 km north west of Paris. This

Table 2
Experimental setup data specific to injections performed on the Brévilles spring test site ($\underline{v}_D$: Darcy's flow; Q_{cr}: critical value of injection rate; M_{inj}: mass tracer injected; V_{inj}: volume tracer injected; C_{inj}: tracer concentration in the injection solution; Q_{inj}: injection rate; Q_{rec}: recirculation rate)

		Pz4			Pz19			Pz17b					Pz17c			
Borehole depth (m)		28			28.4			16					21			
Water column h_w (m)		14.31			9.93			5.81					11.07			
Well radius r_w (m)		0.040			0.040			0.040					0.040			
Well volume V_w (m^3)		0.071			0.078			0.030					0.051			
Screen length e_{scr} (m)		8.9			11.9			2.9					2.9			
K_{mean} (pumping test) (m s^{-1})		2.75×10^{-4}			4.00×10^{-4}			8.67×10^{-4}					2.75×10^{-4}			
Estimated $\underline{v}D$ (m s^{-1})		1.1×10^{-5}			1.5×10^{-5}			1.9×10^{-5}					0.6×10^{-5}			
Estimated Q_{cr} (m^3 s^{-1})		2.6×10^{-5} (93.6 l h^{-1})			4.6×10^{-5} (165.6 l h^{-1})			1.5×10^{-5} (54.0 l h^{-1})					4.7×10^{-6} (16.9 l h^{-1})			
Tracer		Li^+			Sulforhodamine B			I^-					Uranine			
Total M_{inj} (kg)		6.6			10			19.2					5			
Total V_{inj} (m^3)		0.16			0.098			0.16					0.045			
C_{inj} (kg m^{-3})		41.3			102.0			120.0					111.1			
Q_{rec} (m^3 h^{-1})		≈1.0			≈1.0			≈1.0					≈1.0			
	Injection step	1	2	Total	1	2	Total	1	2	3	4	Total	1	2	3	Total
Injection parameters	Q_{inj} (l h^{-1})	23.5	40.9		23.5	35.3		9.4	21.4	32.6	39.9		5.8	15.9	32.6	
	Time (min)	79	51	130	82	99	181	59	35	30	25	149	101.5	31	16	149
	Volume (m^3)	0.031	0.035	0.066	0.032	0.066	0.098	0.009	0.013	0.016	0.017	0.055	0.010	0.008	0.009	0.027
	Tracer mass (kg)	1.28	1.45	2.73	3.26	6.73	10.00	1.08	1.56	1.92	2.04	6.60	1.11	0.88	0.99	2.98
Results	Calculated $\underline{v}D$ (m.s^{-1})		9.8×10^{-6}		1.0×10^{-5}–3.0×10^{-5}					2.5×10^{-5}				4.0×10^{-5}		
	Calculated Q_{cr} (m^3 s^{-1})		2.18×10^{-5} (78.5 l h^{-1})		3.01×10^{-5}–9.04×10^{-5} (108.4–325.4 l h^{-1})					1.82×10^{-5} (65.5 l h^{-1})				2.91×10^{-5} (104.8 l h^{-1})		

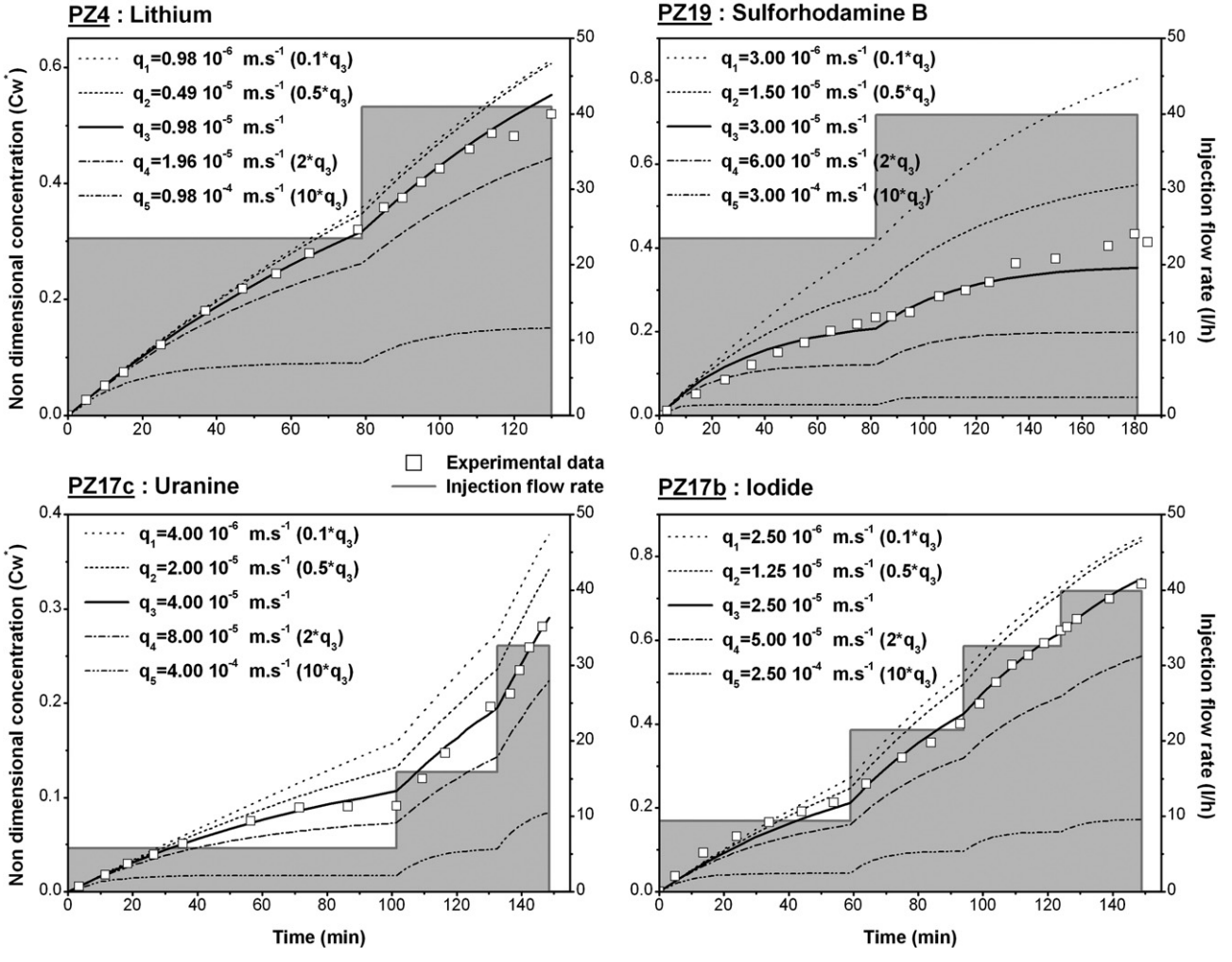

Fig. 7. Monitored and modelled concentration evolution and injection flow rates (Brévilles spring test site experiments).

catchment has been studied for years by BRGM because of a problem with atrazine at the spring (Morvan et al., 2006; Roulier et al., 2006). The aquifer is mainly located in the Cuisian sandy formation limited at its base by a low permeability clay (Fig. 6). These sands are medium in the upper part of the formation to very fine in the lower part. The aquifer system is assumed unconfined and extends over approximately 11.6 km^2. Several springs are observed along the boundary between the sands and the clay. The Brévilles spring is the most important of them and it is considered as the main outlet of the aquifer (Fig. 6).

4.2.1. Description of the injections

Four tracer injections were performed in November 2005, in PZ4, PZ19, PZ17b and PZ17c (Fig. 6). All the details about these injections are provided in Table 2. PZ4 is screened in the lower part of the aquifer where the flow is assumed to be slower. PZ19 is screened over the whole thickness of the aquifer. PZ17 consists of three piezometric boreholes about 2 m distant from each other. The three boreholes are screened at 3 different levels in the aquifer, in the Lutetian limestone lying above the sands (PZ17a), in the upper (PZ17b) and in the lower part (PZ17c) of the Cuise sands, respectively. Tracer quantities were defined to increase the chances of detecting the tracers at the Brévilles spring, which explains the high tracer concentrations that could appear atypical and unnecessarily high for a single FVPDM monitoring. For each experiment, successive steps of constant injection rate were performed. During each injection, samples were collected in the injection well at an approximate frequency of 1 sample every 5 min. Generally, 2 to 4 injection steps were performed, after which the remaining quantity of tracer was injected in a short time to finalize the tracer injection in a reasonable time.

Table 2 presents data on the tracer injections and the technical characteristics of the injection wells. Fig. 7 shows the injection steps together with the concentration evolutions in the four injection wells.

4.2.2. Modelling results

Simulated concentrations were adjusted by modifying only the apparent Darcy flux v_{ap}. The other terms appearing in Eq. (1) were defined based on the experimental conditions only (Q_{inj}, C_{inj}, V_w,...).

Fig. 7 allows comparison of monitored concentrations and adjusted concentrations, using the FVPDM method. In each diagram, the solid thick curve corresponds to the best adjustment of Darcy flux ($v_{ap}=q_3$). The other curves were calculated for v_{ap} equal to $10\times q_3$, $2\times q_3$, $0.5\times q_3$ and $0.1\times q_3$, respectively, to check the sensitivity of the method to the magnitude of the Darcy flux. Fig. 7 shows that the calculated curves almost perfectly match experimental data. Small differences can however be observed for PZ19 probably due to the difficulty in controlling injection conditions because of the very high tracer concentration required. There were problems to keep the concentration of the tracer fluid perfectly homogeneous in the container. It is thus possible that, during the first injection steps, the tracer concentration in

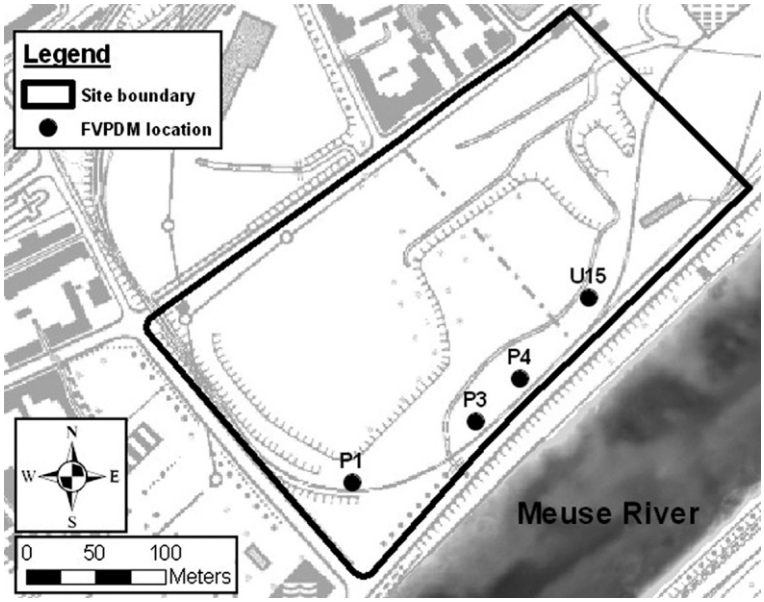

Fig. 8. Location map of wells used in field tracer injections in site A.

Table 3
Characteristics of wells used during injections and experimental set-up characteristics of tracer injections performed in site A ($\underline{v}_D$: Darcy's flow; Q_{cr}: critical value of injection rate; M_{inj}: mass tracer injected; V_{inj}: volume tracer injected; C_{inj}: tracer concentration in the injection solution; Q_{inj}: injection rate; Q_{rec}: recirculation rate)

		U15				P4					P3			P1		
Borehole depth (m)		14.2				15.5					15.0			18.2		
Water column h_w (m)		6.66				7.32					7.03			10.11		
Well radius r_w (m)		0.05				0.075					0.075			0.075		
Well volume V_w (m^3)		0.05				0.13					0.12			0.18		
Screen length e_{scr} (m)		3.0				5.5					4.25			4.25		
K_{mean} (pumping test) (m s^{-1})		3.3×10^{-3}				1.1×10^{-3}					4.0×10^{-4}			2.7×10^{-4}		
Estimated $\underline{v}D$ ($m.s^{-1}$)		1.1×10^{-5}				4.8×10^{-6}					9.8×10^{-7}			5.6×10^{-7}		
Estimated Q_{cr} (m^3 s^{-1})		1.1×10^{-5} (39.6 l h^{-1})				1.3×10^{-5} (46.8 l h^{-1})					1.9×10^{-6} (6.84 l h^{-1})			1.1×10^{-6} (3.96 l h^{-1})		
Tracer		Br^-				I^-					Sluforhodamine B			Uranine		
Total M_{inj} (kg)		2.69				2.77					4.45×10^{-5}			4.25×10^{-5}		
Total V_{inj} (m^3)		0.46				0.98					0.50			0.50		
C_{inj} (ppm)		5818				2775					0.088			0.085		
Q_{rec} (m^3 h^{-1})		0.3				3.0					1.0			0.3		
	Injection step	1	2	3	Total	1	2	3	4	Total	1	2	Total	1	2	Total
Injection parameters	Q_{inj} (l h^{-1})	9.3	32.9	20.3		1.5	5.4	19.2	39.4		1.7	22.8		10.5	20.1	
	Time (h)	3.00	9.58	5.92	18.50	23.4	12.62	20.73	12.30	69.05	29.37	19.83	49.20	19.08	14.92	34.00
	Volume (m^3)	0.028	0.315	0.120	0.463	0.035	0.068	0.398	0.485	0.986	0.050	0.450	0.500	0.200	0.300	0.500
	Tracer mass (kg)	0.16	1.83	0.70	2.69	0.10	0.19	1.12	1.36	2.77	4.4×10^{-6}	4.0×10^{-5}	4.4×10^{-5}	1.7×10^{-5}	2.5×10^{-5}	4.2×10^{-5}
Results	Darcy's flow V_D ($m.s^{-1}$)	$2.05 - 3.1\times10^{-4}$				2.7×10^{-5}						1.5×10^{-5}			3.0×10^{-6}	
	Calculated Q_{cr} ($m^3.s^{-1}$)	1.93×10^{-4}–2.92×10^{-4} (694.8–1051.2 l h^{-1})				7.0×10^{-5} (252.0 l h^{-1})						3.02×10^{-5} (108.7 l h^{-1})			6.02×10^{-6} (21.6 l h^{-1})	

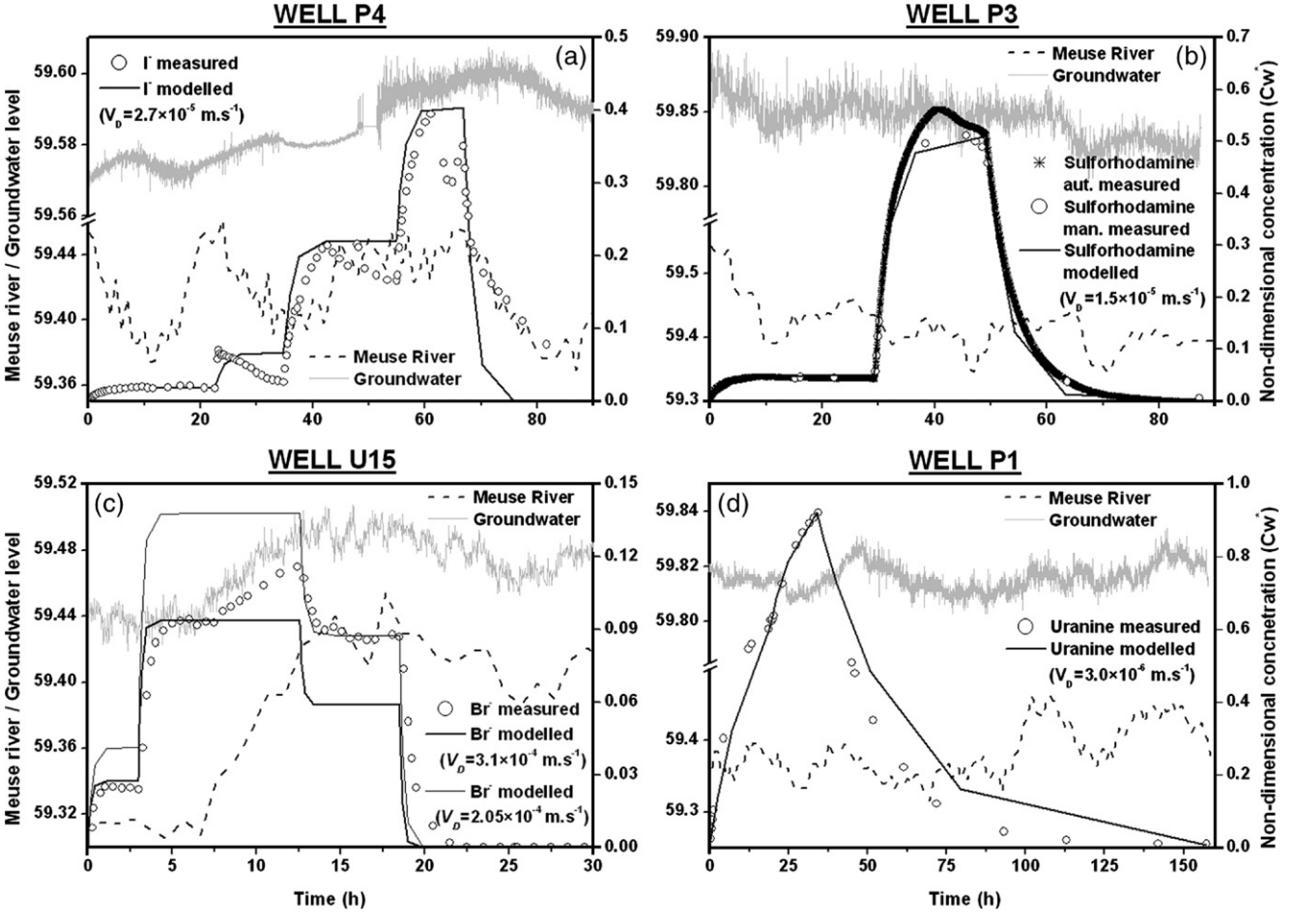

Fig. 9. Comparison between concentration evolutions monitored and modelled in site (V_D is the Darcy's flow) and representation of the Meuse River level and groundwater level in site A.

the injected fluid was lower than expected, the remaining quantity of tracer being injected afterwards.

All the adjustment results are summarized in Table 2. The Darcy fluxes estimated using the FVPDM technique are in good agreement with a priori estimates obtained using the pumping test results and the application of Darcy's law between the injection point and the spring.

4.3. Experimental validation in a brownfield test site (Walloon Meuse basin, Belgium)

The brownfield under investigation corresponds to a former cokery whose activities during the 20th Century have heavily contaminated the soil, subsoil, alluvial deposits and groundwater. The main aquifer is located in the fluvial gravels sediments deposited by the Meuse River overlying the low permeability carboniferous substratum made of shale and sandstone, from 7 m depth to the bedrock (~14 m depth). The topography is flat and the mean hydraulic gradient is low with a value approximately equal to 0.1%.

This test site has been the subject of many investigations during the last 15 years. In this context, many complementary investigations have been performed: borehole drilling, soil and subsoil sampling, hydrogeological investigations such as groundwater monitoring, pumping tests, infiltration tests, etc. This site being fenced, protected and very well equipped (power supply, water available etc), it was possible to define a more advanced protocol and experimental device than in Brévilles.

Various tracer experiments were performed at the site, including FVPDM tests performed in 4 observation wells (U15, P4, P3 and P1) located at the border of the site, at distances ranging from 30 m to 50 m to the Meuse River (Fig. 8). The characteristics of the injection wells are summarized in Table 3.

4.3.1. Description of the injections

Tracer solutions were stored in 500 l barrels. At this site, the volume of tracer fluid and the injection durations were determined to optimize the chances of reaching the stabilization of concentration in the injection well for each injection step, as explained in Fig. 4. Tracers were continuously injected and monitored in each well during several days. Iodide was injected in well P4 using four steps of increasing injection rates, sulforhodamine B in well P3 using two steps of increasing injection rates, bromide in well U15 using two steps of increasing injection rates followed by one step with a decreased injection rate, and uranine in the well P1 using two steps of increasing injection rates. The characteristics of each injection are summarized in Table 3.

With the saline tracers (iodide and bromide), the evolution of concentration was continuously monitored by measuring the electrical conductivity with a YSI 600 XLM probe in the circulation water compared to the electrical conductivity measured in the injection fluid. With fluorescent tracers, a field fluorometer (GGUN-FL30 #1370) was used to monitor the evolution of concentration during the experiment. During each experiment, samples were also taken using an ISCO 6700 automatic sampler and manually (control samples) in order to be analyzed in the laboratory. Groundwater level and temperature were also continuously monitored in the injection wells (every 2 min) using a pressiometric TrollLevel probe.

Fig. 9 shows the concentration evolutions in the injection wells during and after the tracer injections, together with water levels monitored in the injection well and in the Meuse River. Most often, the various injection steps were clearly identifiable, but the monitored concentrations in the injection wells hardly reached stability, as expected by the FVPDM theory for long-duration injections. The reason is that the injection wells are very near the Meuse River and river stage variations generate a pressure wave which is propagated into the aquifer (Workman et al., 1997; Barlow and Moench, 1998; Barlow et al., 2000; Srivastava et al., 2006), as revealed by the continuous monitoring of groundwater and surface water levels performed in the test site. River stage variations generate indirectly local changes in the hydraulic gradients in the aquifer and thus changes in groundwater fluxes close to the injection wells. This phenomenon was observed during most of the injection experiments. During the "transient" phase of the evolution of concentration in the injection well, at the beginning of each tracer injection step, the influence of the changes in groundwater fluxes is not as visible because it overlaps with the "normal" rise of concentration. On the contrary, when the tracer concentration has stabilized in the injection well, changes in groundwater fluxes induce variations in the transit flow rate across of the screens and thus variations in the tracer concentration in the well. This perturbation is clearly visible when looking at the concomitant changes in water levels in the Meuse River and the "anomalies" in concentration monitored in the injections wells. In Fig. 9a and in the second injection step of the Fig. 9b, the observed decreases in Meuse levels are systematically associated with observed decreases in concentrations in the well because the hydraulic gradient and Darcy fluxes are increased in the vicinity of the injection well. On the contrary, during the stabilized phase

of the second step of bromide injection in well U15 (Fig. 9c), an increase in tracer concentration is observed, corresponding to a rise in water levels in the Meuse because the hydraulic gradient and Darcy fluxes are reduced close to U15.

4.3.2. Modelling results

Using Eq. (1), calculated evolutions of concentrations were fitted to the monitored ones by modifying the apparent Darcy flux v_{ap} (Fig. 9). Similar to Brévilles tests, all other terms appearing in Eq. (1) were defined based on the experimental conditions (Q_{inj}, C_{inj}, V_w …). The results are summarized in Table 3. Considering that the influence of changes in water levels in the Meuse was not taken into account directly in the interpretation, one can consider that tracer concentration evolutions calculated with the analytical solution are very close to the measured ones. As explained before, for the injection performed in U15, the strong deviation of concentration observed during injection in step 2 is related to a rise of about 15 cm in the Meuse water level during the FVPDM experiment. For a Darcy flux of 3.1×10^{-4} m s^{-1}, the first injection step and the beginning of the second step are well reproduced, but not the third for which the calculated concentration is too low. These results are consistent with the fact that the rise in Meuse water level has reduced the gradient and thus Darcy fluxes in the gravel aquifer near the river bank. The third step was adjusted separately, using a lower Darcy flux equal to 2.05×10^{-4} m s^{-1}.

The estimated Darcy fluxes are similar in P3 and P4, on the order of 2×10^{-5} m s^{-1} while in the vicinity of well P1, they are 10 times lower, around 3×10^{-6} m s^{-1}. In the vicinity of well U15, the estimated Darcy flux is approximately 10 times higher of those in P3 and P4, of the order or 2×10^{-4} m s^{-1}. This seems to indicate a zone of higher hydraulic conductivity in the region of U15.

4.4. Possible limitations of the FVPDM

The two case studies where the FVPDM was applied indicate that it is applicable in a large range of contexts. However, two limitations should be mentioned. Because of the water circulation required in the injection well for the homogenization of the tracer concentration and for sampling, the FVPDM can not be used for profiling groundwater fluxes along well screens, contrary to the PDM. It is also likely that the FVPDM technique would be more difficult to apply in large or very deep wells where the homogenization of concentration would not be evident because the turnover of water in the well bore would be long. However, developments are on the way to develop the use of the FVPDM in deep wells, as a tracer-based well logging technique, where the water circulation system is progressively moved along the well axis.

5. Conclusions and perspectives

One of the main outcomes of this research is the development of a new tracer technique for the quantification of Darcy fluxes in groundwater. The mathematical framework has been described and discussed in detail and, from a more practical point of view, detailed guidelines are provided in the experimental setup of the technique, derived from the sensitivity analysis of a non-dimensional formulation of the model. This technique can be used as a "stand-alone" single-well tracer experiment or in combination with any other tracer technique, in which case it can provide a control of injection conditions together with complementary information on groundwater flows in the vicinity of the injection well.

The two case studies presented show that the FVPDM technique has a wide range of applications where the quantification of Darcy fluxes is required, for very contrasting objectives and experimental conditions. For the two case studies, the results indicate that the technique is very robust, reliable and sensitive to groundwater flow conditions. The interpretation can take advantage of both the rising and the stabilized part of the concentration evolutions in the injection well.

As a consequence of its high sensitivity to experimental conditions, the FVPDM is also a candidate technique for studying and monitoring changes in Darcy fluxes and groundwater flows in transient conditions, such as changes in hydraulic gradients, with potential applications in monitoring the dynamics of groundwater — surface water interactions in the hyporheic zone. To do so, one needs to continuously inject a tracer at a very low rate and to monitor the temporal changes in concentration in the injection well. The analytical solution could be straightforwardly extended to account for dynamically changing Darcy fluxes and volumes of water in the injection well.

It would also be very interesting to see if the FVPDM interpretation can not be improved by interpreting the long-term behaviour of the tracer concentration evolution in the injection well using asymptotic approaches, such as those proposed by Jaekel et al. (1996), Vasco and Datta-Gupta (1999), Vereecken et al. (1999a,b) or Haggerty et al. (2000). This improvement could provide useful complementary information on the physico-chemical behaviour of the tracer in the aquifer. The FVPDM could also be efficiently combined to passive flux meters (Hatfield et al., 2004) for a better assessment

of cumulated groundwater fluxes at the vicinity of the monitored well.

A Fortran 90 programme was written in order to calculate the concentration evolution in the injection well and the actual tracer input function in the aquifer for arbitrary tracer injection configurations. It is available from the corresponding author upon request.

Notation and units

C_{in} variable accounting for the concentration in any injected fluid (generic notation) [M L^{-3}]
C_{inj} tracer concentration in the injected fluid during tracer injection [M L^{-3}]
C_t variable accounting for the tracer concentration in the transit flux intercepted by the well screens [M L^{-3}]
C_w variable accounting for the tracer concentration in the injection well [M L^{-3}]
$C_{w,0}$ initial concentration of tracer in the injection well [M L^{-3}]
$C_{w,e_{\text{inj}}}$ residual tracer concentration in the injection well at the end of the injection of the tracer fluid [M L^{-3}]
$C_{w,e_{\text{fl}}}$ residual tracer concentration in the injection well at the end of the flushing operations [M L^{-3}]
$C_{w,\text{stab}}$ stabilized concentration in the well [M L^{-3}]
C_{DL} tracer concentration representing the device detection limit [M L^{-3}]
C_{SL} tracer concentration representing the device saturation limit [M L^{-3}]
e_{scr} length of the well screens [L]
h_w height of the water column in the well bore [L]
M_{inj} mass of tracer injected in the well [M]
Q_{cr} critical injection flow rate [L^3 T^{-1}]
Q_{in} variable accounting for the any injection flow rate (generic notation) [L^3 T^{-1}]
Q_{inj} injection flow rate during tracer injection operations [L^3 T^{-1}]
Q_{fl} injection flow rate during flushing operations [L^3 T^{-1}]
Q_{out} flow rate leaving the well through the screens [L^3 T^{-1}]
Q_t^0 transit flow rate across the well screens under natural groundwater flow conditions [L^3 T^{-1}]
Q_t^{in} variable accounting for the transit flow rate intercepted by the well screens as a function of the injection rate Q_{in} (generic notation) [L^3 T^{-1}]
r_w radius of the injection well [L]
T_{inj} tracer injection duration [T]
T_{fl} water flush duration [T]
T_w time needed to replace the water in the well at the critical injection flow rate [T]
v_{ap} apparent Darcy flux prevailing in the aquifer, as measured in the injection well [L T^{-1}]
v_D Darcy flux prevailing in the aquifer without the distorting influence of the injection well [L T^{-1}]
v_r radial Darcy flux (in a coordinates system centred on the well) [L T^{-1}]
v_θ tangential Darcy flux (in a coordinates system centred on the well) [L T^{-1}]
V_{in} variable accounting for any volume of injected fluid (generic notation) [L^3]
V_{inj} volume of tracer fluid injected in the well [L^3]
V_{fl} volume of water flush injected in the well after tracer injection [L^3]
V_w volume of water in the injection well [L^3]
V_w^{mix} mixing volume of water usually equal to V_w [L^3]
V_t volume of water intercepted by the screen of the well during tracer injection [L^3]
α_w distortion coefficient accounting for the discontinuity introduced in the flow field by the injection well bore [−]

Non-dimensional formulations:

$$C^* = \frac{C}{C_{\text{inj}}},\ Q^* = \frac{Q}{Q_{\text{cr}}},\ V^* = \frac{V}{V_w},\ t^* = \frac{t}{T_w}$$

Acknowledgements

This work was supported by the European Union FP6 Integrated Project AquaTerra (Project no. 505428) under the thematic priority, sustainable development, global change and ecosystems and by Research funds provided by Aquapôle-ULg. Mr. B. Belot, from the Laboratory of water analysis of HGULg performed the analyses of lithium and iodide. Dr. Ph. Meus, from the SME "European Water Tracing Services — EWTS", assisted in using the field fluorimeter and performed the analyses of the fluorescent tracers. They are gratefully acknowledged for suggestions and comments on the interpretation of the results. Thanks to the BRGM — Water Division, especially C. Mouvet who gave us the opportunity to work on the Brévilles test site and A. Gutierrez who assisted in the field experiments. Thanks to the SPAQuE, especially H. Halen and A. Lox, for access to data and to the brownfield in the alluvial plain of the Meuse River in Belgium. Thanks are also due to P. Theunissen (SPE-TGV) for his gracious contribution on Meuse data time series. Special thanks to René Therrien for his careful review of the manuscript.

References

Arntzen, E.V., Geist, D.R., Dresel, P.E., 2006. Effects of fluctuating river flow on groundwater/surface water mixing in the hyporheic zone of a regulated, large cobble bed river. River Res. Applic. 22 (8), 937–946.

Australian Government, http://www.connectedwater.gov.au/framework/stream_flow_dilution.php, 2006.

Barlow, P.M., Moench, A.F., 1998. Analytical solutions and computer programs for hydraulic interactions of stream-aquifer systems. USGS, Marlborough, Massachusetts, USA. 99 pp.

Barlow, P.M., DeSimone, L.A., Moench, A.F., 2000. Aquifer response to stream-stage and recharge variations. II. Convolution method and applications. J. Hydrol. 230, 211–229.

Batlle-Aguilar, J., Brouyère, S., 2005. Documentation of site equipment and description of experiments performed and still planned in the former cokery test site A. Deliverable R3.15, AquaTerra (Integrated Project FP6 no. 505428). 22 pp.

Batlle-Aguilar, J., Brouyère, S., 2006. Update on field experiments and description of the groundwater flow and transport model for the cokery site A., AquaTerra (Integrated Project FP6 no. 505428). 50 pp.

Bidaux, P., Tsang, C.-F., 1991. Fluid flow patterns around a well bore or an underground drift with complex skin effects. Water Resour. Res. 27 (11), 2993–3008.

Brouyère, S., 2001. Etude et modélisation du transport et du piégeage des solutés en milieu souterrain variablement saturé (Study and modelling of transport and retardation of solutes in variably saturated media). Faculté des Sciences Appliquées. Laboratoire de géologie de l'ingénieur, d'Hydrogéologie et de Prospection géophysique. Université de Liège, Liège, Belgium, p. 640 (In French).

Brouyère, S., 2003. Modeling tracer injection and well-aquifer interactions: a new mathematical and numerical approach. Water Resour. Res. 39 (3). doi:10.1029/2002WR001813.

Brouyère, S., Carabin, G., Dassargues, A., 2005. Influence of injection conditions on field tracer experiments. Ground Water 43, 389–400.

Brusseau, M.L., 1994. Transport of reactive contaminants in heterogeneous porous media. Rev. Geophys. 32 (3), 285–313.

Devlin, J.F., McElwee, C.D., 2007. Effects of measurement error on horizontal hydraulic gradient estimates. Ground Water 45 (1), 62–73.

Drost, W., Klotz, D., Arnd, K., Heribet, M., Neumaier, F., Rauert, W., 1968. Point dilution methods of investigation ground water flow by means of radioisotopes. Water Resour. Res. 4 (1), 125–146.

Gilman, K., 1977a. Dilution gauging on the recession limb: 1. Constant rate injection method. Hydrol. Sci. Bull. 22 (3), 353–369.

Gilman, K., 1977b. Dilution gauging on the recession limb: 2. The integration method. Hydrol. Sci. Bull. 22 (4), 469–481.

Goderniaux, P., Brouyère, S., 2006. Report on the tracer tests (experimental setup, results and interpretation). Deliverable H2.3, AquaTerra (Integrated Project FP6 no. 505428). 49 pp.

Haggerty, R., McKenna, S.A., Meigs, L.C., 2000. On the late-time behavior of tracer test breakthrough curves. Water Resour. Res. 36 (12), 3467–3479.

Hall, S.H., 1996. Practical single-well tracer methods for aquifer testing. Tenth National Outdoor Action Conference and Exposition, Columbus, Ohio, USA. Natural Groundwater Association.

Hatfield, K., Annable, M., Cho, J., Rao, P.S.C., Klammler, H., 2004. A direct passive method for measuring water and contaminant fluxes in porous media. J. Contam. Hydrol. 75, 155–181.

Havely, E., Moser, H., Zellhofer, O., Zuber, E., 1967. Borehole dilution techniques: a critical review. Isotopes in Hydrology. I.A.E. A., Vienna, Austria.

Jaekel, U., Georgescu, A., Vareecken, H., 1996. Asymptotic analysis of nonlinear equilibrium solute transport media. Water Resour. Res. 32 (10), 3039–3098.

Kalbus, E., Reisntorf, F., Schirmer, M., 2006. Measuring methods for groundwater–surface water interactions: a review. Hydrol. Earth Syst. Sci. 10, 873–887.

Klotz, D., Moser, H., Trimborn, P., 1978. Single-borehole techniques; present status and examples of recent applications. Symposium IAEA, Neuherberg, Germany.

Li, L., Barry, D.A., Culligan-Hensley, P.J., Bajracharya, K., 1994. Mass transfer in soils with local stratification of hydraulic conductivity. Water Resour. Res. 30 (11), 2891–2900.

Morrison, S.J., Metzler, D.R., Dwyer, B.P., 2002. Removal of As, Mn, Mo, Se, U, V and Zn from groundwater by zero-valent iron in a passive treatment cell: reaction progress modeling. J. Contam. Hydrol. 56, 99–116.

Morvan, X., Mouvet, C., Baran, N., Gutierrez, A., 2006. Pesticides in the groundwater of a spring draining a sandy aquifer: temporal variability of concentrations and fluxes. J. Contam. Hydrol. 87, 176–190.

Roulier, S., Baran, N., Mouvet, C., Stenemo, F., Morvan, X., Albrechtsen, H.J., Clausen, L., Jarvis, N., 2006. Controls on atrazine leaching through a soil-unsaturated fractured limestone sequence at Brévilles, France. J. Contam. Hydrol. 84, 81–105.

Ruehl, C., Fisher, A.T., Hatch, C., Los Huertos, M., Stemler, G., Shennan, C., 2006. Differential gauging and tracer tests resolve seepage fluxes in a strongly-losing stream. J. Hydrol. 330, 235–248.

Srivastava, K., Serrano, S.E., Workman, S.R., 2006. Stochastic modeling of transient stream-aquifer interaction with the nonlinear Boussinesq equation. J. Hydrol. 328, 538–547.

Valocchi, A.J., 1985. Validity of the local equilibrium assumption for modelling sorbing solute transport through homogeneous soils. Water Resour. Res. 21 (6), 808–820.

Vasco, D.W., Datta-Gupta, A., 1999. Asymptotic solutions for solute transport: A formalism for tracer tomography. Water Resour. Res. 35 (1), 1–16.

Vereecken, H., Jaekel, U., Esser, O., Nitzsche, O., 1999a. Solute transport analysis of bromide, uranin and LiCl using breakthrough curves from aquifer sediment. J. Contam. Hydrol. 39, 7–34.

Vereecken, H., Jaekel, U., Georgescu, A., 1999b. Asymptotic analysis of solute transport with linear nonequilibrium sorption in porous media. Transp. Porous Media 36, 189–210.

Workman, S.R., Serrano, S.E., Liberty, K., 1997. Development and application of an analytical model of stream/aquifer interaction. J. Hydrol. 200, 149–163.

Wroblicky, G.J., Campana, M.E., Valett, H.M., Dahm, C.N., 1998. Seasonal variation in surface–subsurface water exchange and lateral hyporheic area of two stream-aquifer systems. Water Resour. Res. 34 (3), 317–328.